clinical and translational neuroscience

MDPI

Article

Clinical Phenotype Imprints on Brain Atrophy Progression in Parkinson's Disease

David H. Benninger [1,*], Jan von Meyenburg [2], Juergen Dukart [3,4], Claudio L. Bassetti [5], Spyridon S. Kollias [2], Kazumi Iseki [6] and Bogdan Draganski [1,7,8,*]

1 Service of Neurology, Department of Clinical Neurosciences, Centre Hospitalier Universitaire Vaudois Lausanne, University of Lausanne, 1011 Lausanne, Switzerland
2 Neuroradiology Clinic, University Hospital Zürich, 8091 Zürich, Switzerland
3 Institute of Neuroscience and Medicine, Brain and Behaviour (INM-7), Research Centre Jülich, 52428 Jülich, Germany
4 Institute of Systems Neuroscience, Medical Faculty, Heinrich Heine University Düsseldorf, 40225 Düsseldorf, Germany
5 Department of Neurology, University Hospital of Bern, 3010 Bern, Switzerland
6 Department of Neurology, Fujimoto Hospital, Neyagawa, Osaka 583-0857, Japan
7 LREN, Department of Clinical Neurosciences, University of Lausanne, CHUV, 1011 Lausanne, Switzerland
8 Max Planck Institute for Human Cognitive and Brain Sciences, 04103 Leipzig, Germany
* Correspondence: david.benninger@chuv.ch (D.H.B.); bogdan.draganski@chuv.ch (B.D.); Tel.: +41-21-314-95-83 (D.H.B.); +41-21-314-96-38 (B.D.); Fax: +41-21-314-12-56 (D.H.B. & B.D.)

Abstract: There is much controversy about the link between motor symptom progression and the plethora of reported brain atrophy patterns in idiopathic Parkinson's disease (PD). The main goal of this study is to provide empirical evidence for unique and common contributions of clinical phenotype characteristics on the dynamic changes of brain structure over time. We analyzed the behavioral and magnetic resonance imaging (MRI) data of PD patients (n = 22) and healthy individuals (n = 21) acquired two years apart through the computational anatomy framework of longitudinal voxel-based morphometry (VBM). This analysis revealed a symmetrical bi-hemispheric pattern of accelerated grey matter decrease in PD extending through the insula, parahippocampal gyrus, medial temporal lobes and the precuneus. We observed a hemisphere-specific correlation between the established scores for motor symptoms severity and the rate of atrophy within motor regions, which was further differentiated by the clinical phenotype characteristics of PD patients. Baseline cerebellum anatomy differences between the tremor-dominant and akineto-rigid PD remained stable over time and can be regarded as trait rather than state-associated features. We interpret the observed pattern of progressive brain anatomy changes as mainly linked to insular areas that determine together with basal ganglia the motor and non-motor phenotype in PD. Our findings provide empirical evidence for the sensitivity of computational anatomy to dynamic changes in PD, offering additional opportunities to establish reliable models of disease progression.

Keywords: idiopathic Parkinson's disease; basal ganglia; UPDRS; longitudinal study; tissue probability maps; voxel-based morphometry

Citation: Benninger, D.H.; von Meyenburg, J.; Dukart, J.; Bassetti, C.L.; Kollias, S.S.; Iseki, K.; Draganski, B. Clinical Phenotype Imprints on Brain Atrophy Progression in Parkinson's Disease. *Clin. Transl. Neurosci.* **2023**, *7*, 8. https://doi.org/10.3390/ctn7010008

Academic Editor: Karl-Olof Lovblad

Received: 31 January 2023
Revised: 24 February 2023
Accepted: 26 February 2023
Published: 28 February 2023

1. Introduction

The progression of idiopathic Parkinson's disease (PD) is characterized by motor and non-motor deficits that pose significant therapeutic challenges in the due course of the disease [1]. The observed inter-individual heterogeneity in clinical phenotype progression is considered to reflect the spatial distribution of pathology spread, as suggested by human and non-human primate models of PD [2].

As the current knowledge of PD progression is limited to clinical observations compromised by inter-individual variability and changes in dopaminergic treatment dosage, there is a need to identify biomarkers reflecting the impact of the pathological process,

which could be linked with subject-specific symptom progression [3]. Computational anatomy using structural MRI and sophisticated voxel- or surface-based algorithms allows the extraction of characteristic brain features that offer an unprecedented opportunity to track the in vivo trajectories of grey matter volume or cortical thickness changes in the due course of healthy ageing and neurodegeneration. While many computational anatomy studies in healthy ageing and the advanced stages of various neurodegenerative diseases show robust results, in PD, there is substantial controversy that underscores the difficulty of standardizing study populations.

Already published longitudinal studies in PD showed differential patterns in patients with cognitive impairment [4]; they failed, however, to demonstrate correlation with an individual's degree of motor impairment [5–8]. A more recent milestone study spanning an observation period of more than 8 years showed widespread atrophy patterns across the insula, inferior parietal lobule, occipital and temporal lobes and concluded that the computational anatomy of longitudinal MRI data reliably captures the established Braak stages in patients with idiopathic Parkinson's disease [9]. Methodological differences in MRI data processing and analysis are discussed as the main reason for the disparity of presented results. Particularly puzzling is the fact that the majority of longitudinal studies almost exclusively show only cortical changes over time, except two morphometry investigations demonstrating basal ganglia changes [10,11]. This is due to the fact that automated tissue classification relies on the distribution of image intensities and grey–white matter contrast in MRI images [12], which are determined by the local values of the MRI parameters and the microstructural composition of brain tissue. In particular, the inaccurate classification of subcortical structures from T1-weighted (T1w) images—the most widely used data in computational anatomy, arises from the high concentration of iron in these regions [13].

The objective of our study was to assess the PD-related pattern of brain atrophy with emphasis on clinical phenotype in a longitudinal study over 2 years. We hypothesized that the progression of motor and non-motor symptoms in PD patients over time will result in the differential patterns of brain structure changes involving associative, sensorimotor and limbic areas. More specifically, the supposition here is that PD patients will show a more rapid grey matter loss compared with the estimated trajectories of healthy ageing. Along these lines, we predict a strong correlation between these dynamic changes in brain structure and the clinical metrics of symptom severity, in addition to the observed predominance of tremor phenotype or akineto-rigid phenotype. To this aim, we analyzed clinical phenotype characteristics together with longitudinal MRI data that were acquired two years apart and processed with dedicated software, which provided optimal feature extraction accuracy in both cortical and subcortical areas.

2. Materials and Methods

2.1. Study Population

We recruited 27 patients with mild to moderate PD corresponding to Hoehn and Yahr stages (HY) 2–3. From these, 2 declined participation, 2 did not attend the follow-up exam, 1 was deemed MRI incompatible due to a cardiac pacemaker, which resulted in 22 male individuals (age 57–71 years; mean age 63.5 $\pm$ 4.3 years) who were included in the final analysis. The healthy control cohort consisted of 21 randomly selected participants (17 males, aged 33–77 years, mean age 62.1 $\pm$ 11.6 years) from the Parkinson's Progression Marker Initiative (PPMI) and the Alzheimer's Disease Neuroimaging Initiative (ADNI), with MRI scanning performed two years apart on a 3T MRI scanner (www.loni.ucla.edu/ADNI, accessed on 12 May 2016; www.ppmi-info.org).

PD diagnosis was based on UK PD Brain Bank criteria [14] with a minimum disease duration of 3 years. Exclusion criteria were advanced PD stages equivalent to HY 4–5, secondary Parkinsonism and atypical Parkinsonism. Additionally, we excluded individuals with dementia, as defined by a score < 24 in the mini-mental state examination; any structural pathology in brain MR and CT imaging; previous stereotactic surgery; and

medical or psychiatric conditions precluding study participation and/or performance of MRI.

Patients with tremors were defined to have a typical Parkinsonian resting tremor with or without postural or action tremor of similar frequency without evidence of another origin. Patients without tremor were classified separately after the exclusion of resting, postural or action tremor. Within the PD cohort, 12 of the 22 (55%) had a classical parkinsonian resting tremor.

All patients provided written informed consent for study participation, which was approved by the local ethics committee.

2.2. Clinical Assessment

All patients underwent a detailed clinical assessment. To assess the severity of the rest tremor, we obtained a composite tremor score, covering the previous 6 months, and using a similar scale as in UPDRS (0—absent; 1—mild and infrequent, not bothersome; 2—moderate and bothersome; 3—severe and interfering with many activities; and 4—marked and interfering with most activities).

The detailed neuropsychological evaluation included a handedness questionnaire, the mini-mental state examination—MMSE; verbal and figural (5-point test) fluency; Rey auditory verbal learning test—RAVLT; Rey visual design learning test—RVDLT; and the complex figure test and the Stroop interference test. We also screened for other cognitive deficits, such as apraxia, aphasia and agnosia. Depression was considered present if either one or both cut-offs of 14/15 and 12/13 in the Beck depression inventory (BDI) and the Hamilton depression rating scale (HAMD), respectively, were exceeded. Details regarding the clinical tests performed in the ADNI and PPMI cohorts and assuring the absence of manifest brain disorders can be found elsewhere.

2.3. Brain MRI

MR imaging was performed with a 3T MR-scanner (PHILIPS, Achieva) using a standard head coil. Our structural protocol consisted of T1-weighted (T1w), 3D magnetization-prepared rapid gradient-echo (MPRAGE) sequence acquisition (TR = 8.7 ms, TE 2.3 ms, flip angle 8.0°, voxel-size 0.86 × 0.86 × 1.0 mm, axial slice orientation, and matrix size 256 × 256). Images were visually inspected for motion artefacts before pre-processing and redone if deemed necessary.

The MRI dataset of randomly selected healthy controls who were scanned 2 years apart included standard T1w images obtained with different 3T scanners using a 3D magnetization-prepared rapid gradient-echo (MPRAGE) sequence varying in repetition and echo time (www.loni.ucla.edu/ADNI, accessed on 12 May 2016; www.ppmi-info.org).

2.4. MRI Data Pre-Processing

MR images were pre-processed for statistical analysis within the statistical parametric mapping framework (Wellcome Centre for Human Neuroimaging, UCL London UK, SPM12, http://www.fil.ion.ucl.ac.uk/spm, accessed on 18 January 2016.) using basal ganglia optimized tissue priors [15]. The individual images of the two different time points were corrected for magnetic field intensity inhomogeneities and registered to a within-subject mid-point average using non-linear geodesic shooting registration [16]. The algorithm extracts the Jacobian determinants representative of the grey matter volume rate of change with the explicit acknowledgment of time units between the data acquisition time points. We performed the automated tissue classification of the mid-point average images followed by spatial registration using the diffeomorphic registration algorithms of DARTEL [17]. The images representative of the grey matter rate of change were multiplied by the grey matter probability maps, spatially registered to MNI space and spatially smoothed with Gaussian kernel of 8 mm full-width-at-half-maximum.

2.5. Statistical Analysis

The statistical analysis of clinical data was carried out with an SPSS Version 12.0.1 for Windows. The normality of distribution was tested with skewness and kurtosis tests. Unpaired *t*-tests were used to compare parametric data between groups, and Mann–Whitney U tests was used for non-parametric data. Chi-square or Fisher exact tests were used to compare nominal data.

For the between-group statistical comparisons of the rates of grey matter volume change, we used the general linear model implementation in SPM12. We created a factorial design with levels defined by groupings based on clinical phenotype—i) akineto-rigid type on the left; ii) tremor-dominance on the left, iii) akineto-rigid type on the right; and iv) tremor-dominance on the right and healthy controls. We included age, gender and total intracranial volume (TIV) calculated as the sum of grey matter, white matter and cerebro-spinal fluid volume. We also introduced the difference in UPDRS III scores between time point one (TP1) and two (TP2; positive numbers signified improved UPDRS III score), which were modelled separately for the left and the right body side, in addition to the difference between levodopa medication (in levodopa equivalent doses—LED) at time point one and two.

We first tested for grey matter volume differences between cohorts independent from disease progression, using the individuals' maps of mid-point grey matter volume averages as the dependent variable. Using the very same statistical design, we then tested the rate of volume change between the two time-points for the differential effects of motor and cognitive performance on the brain. Results are reported as significant after voxel-wise $p < 0.05$ family-wise error (FWE) correction for multiple comparisons and reported as trends when surviving the threshold of $p < 0.001$, uncorrected for multiple comparisons.

3. Results

3.1. Clinical Phenotype

Motor complications and impaired balance were more prevalent in patients without tremors, who had a higher score for balance and gait (UPDRS items 27–30). No other differences were found, either in scores of bradykinesia (items 18–19, 23–26, 31), rigidity (items 22), single and combined UPDRS parts (I, II, III on and IV "on" data; sparse III "off" data precluded comparison), or with respect to the degree of asymmetry or the laterality of disease preponderance (for demographic and clinical characteristics see Table 1). Resting tremor was bilateral in 10 and unilateral in 2 patients (right, $n = 2$; UPDRS item 20 "on", median 2, range 0–10). Composite rest ± postural and/or action tremor scores were similar in most patients when off medication (moderate, $n = 5$; severe, $n = 6$; marked, $n = 1$).

Compared to age- and sex-matched healthy controls (unpublished data), the neuropsychological assessment of the patients yielded mild impairments in executive functions (figural fluency and concept learning and shifting) and in memory (verbal and figural learning and recall). No significant differences in the neuropsychological test results were found when comparing patients with tremor and akineto-rigid PD.

Table 1. Demographics and clinical findings in PD patients ($n = 22$) and controls ($n = 21$). Comparison between time-points using a paired *t*-test.

	PD Patients			**Controls**		
	TP1	**TP2**	***p***	**TP1**	**TP2**	***p***
Number	22	22	-	21	21	-
Age (years; mean ± SD)	61.7 ± 4.3	63.6 ± 4.3	<0.001 *	60.2 ± 11.7	62 ± 11.7	n.s.
Gender (m:f; count)	22:0			17:4		0.04 **
MMSE (score)	28.5 ± 1.0	28.2 ± 1.4	n.s	29.5 ± 0.6	29.6 ± 0.8	n.s.

Table 1. *Cont.*

	PD Patients			Controls		
	TP1	**TP2**	***p***	**TP1**	**TP2**	***p***
Disease duration (months; mean ± SD)	86.8 ± 47.4	110.8 ± 47.4	<0.001 *	-	-	-
LED (mg; median (range))	1030 (100–1790)	1022 (500–1840)	n.s.	-	-	-
Motor score (UPDRS III) (score; median (range))	26 (12–35)	25 (11–42)	n.s.	-	-	-
Impaired balance (HY ≥ 2.5) (% (*n*))	64% (14)	91% (20)	0.03 *	-	-	-
Balance and Gait (UPDRS items 27–30) (median (range))	4 (0–6)	4 (1–7)	n.s.	-	-	-
Total Intracranial Volume (mm^3; mean ± SD)	1611/15.8			1504/13.9		0.02 **

*—significant differences between time points (TP1-TP2) ($p < 0.05$); **—significant differences between groups ($p < 0.05$); n.s.—not significant.

3.2. Brain Anatomy

Rate of Volume Change

Comparison between PD patients and healthy controls: The differential contrast comparing the rate of grey matter volume change between PD patients and healthy controls showed a significant increase in volume loss in the left anterior insula, right precuneus, right parahippocampal gyrus and left midtemporal gyrus. There were trends for the higher rate of change of the corresponding contralateral cortical areas (Figure 1 and Table 2). For all findings, there were no significant differential contributions of the akineto-rigid subtype compared with tremor-dominant phenotype. The dichotomization of PD patients into two subgroups—the "akineto-rigid" and "tremor" forms—which did not show any significant differences in the rate of volume change, particularly in the area reported in the analysis of progression-independent grey matter volume differences (Supplementary Figure S1 and Supplementary Table S1).

Regression analyses within the PD cohort: The regression analyses used the identical design matrix; however, testing the interaction between changes in the body-side specific motor part of the UPDRS and atrophy rate showed that motor symptom progression is associated with a stronger rate of change in the contralateral primary motor cortex and the frontal and parietal cortex (Figure 2 and Table 3). There were no significant correlations with the cognitive test results—verbal, figurative memory, fluency, recognition or recall.

Cross-sectional analysis within the PD cohort: The comparison of grey matter volume maps generated from the mid-point average images confirmed the trend of the previously reported findings [18] of grey matter loss in the right cerebellum in patients with tremor compared with the akineto-rigid phenotype (Supplementary Figure S1 and Supplementary Table S1).

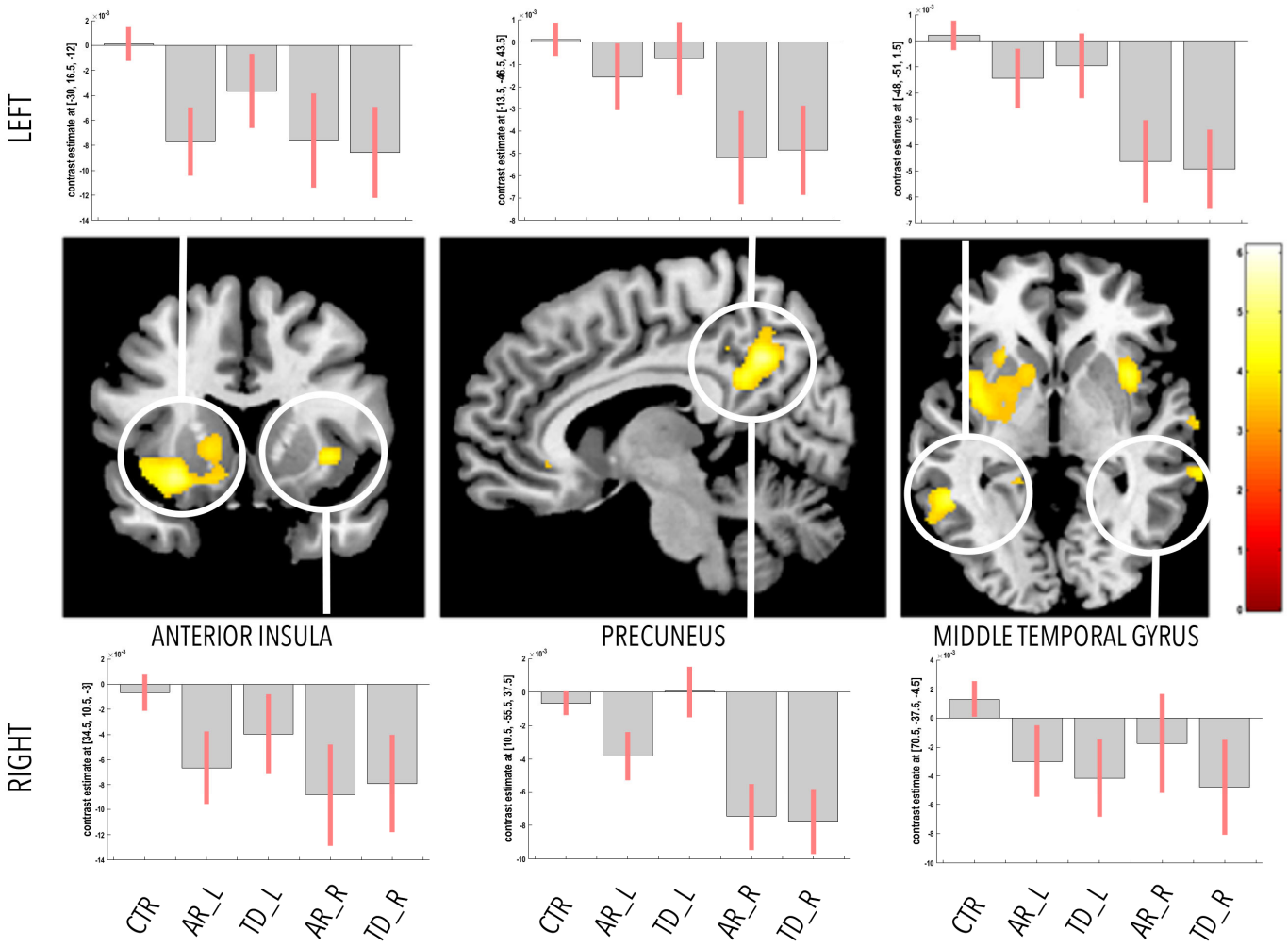

Figure 1. Whole-brain analysis of differential grey matter volume rate of change between akineto-rigid and tremor-dominant forms of PD and healthy controls. Statistical parametric maps with a threshold for presentation purposes at $p < 0.001$, uncorrected for multiple comparisons overlaid on standard T1-weighted image in standard Montreal Neurological Institute space. Bar plots represent the contrast estimates for each subgroup of PD patients and healthy controls. Abbreviations: CTR—healthy controls; AR_L—akineto-rigid symptoms on the left; AR_R—akineto-rigid symptoms on the right; TD_L—tremor-predominance on the left; TD_R—tremor-predominance on the right.

Table 2. Main effects analysis—rate of gray matter volume change.

Main Effects	Region	Side	MNI Coordinates (mm)			*p*-Value (FWE-Corr)
			x	y	z	
PD < HC	Parahippocampal gyrus	R	30	−32	−15	$p = 0.037$
	Parahippocampal gyrus	L	−21	−35	−12	$p = 0.56$ º
	Anterior insula	R	36	9	−2	$p = 0.29$ º
	Anterior insula	L	−30	17	−12	$p = 0.04$
	Precuneus	R	11	−56	38	$p = 0.01$
	Precuneus	L	−14	−44	44	$p = 0.23$ º
	Middle temporal gyrus	R	71	−38	−5	$p = 0.5$ º
	Middle temporal gyrus	L	−48	−51	2	$p = 0.012$

Trends are denoted with a circle o.

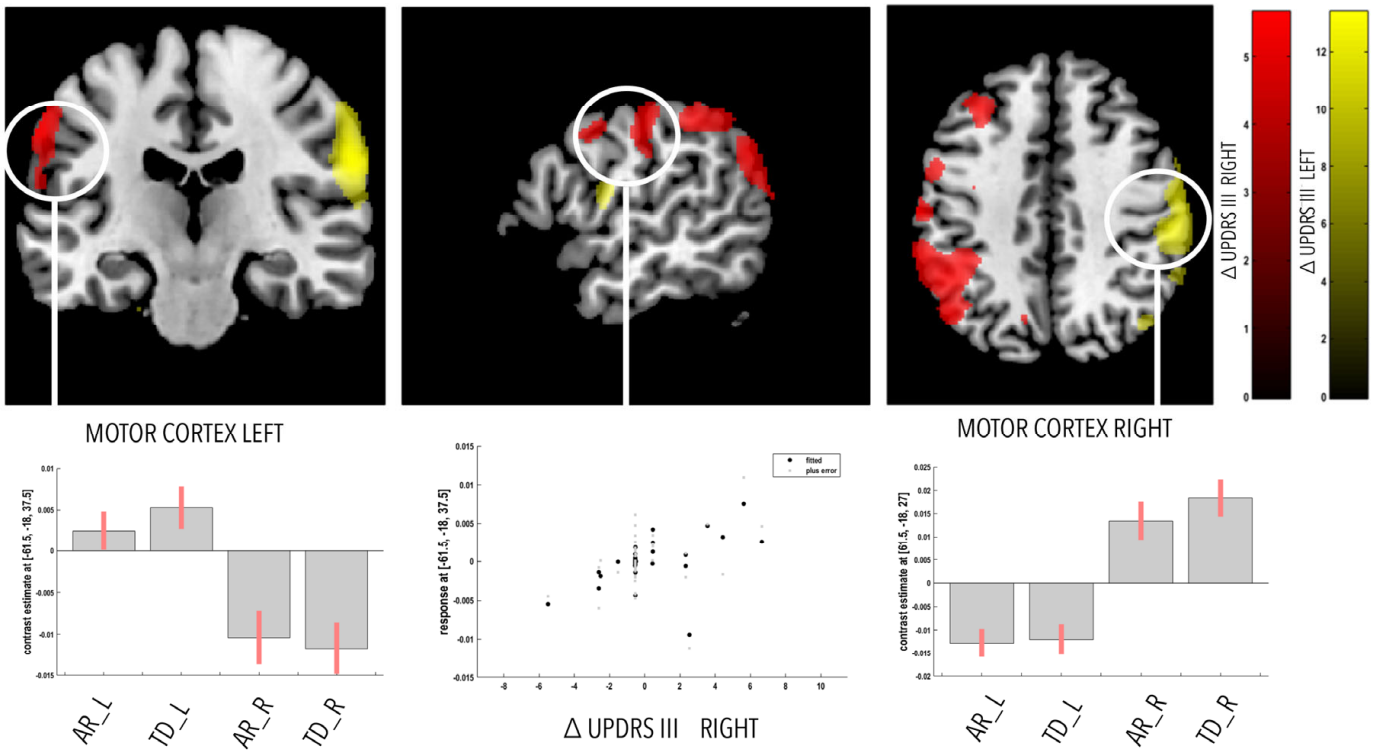

Figure 2. Top: Whole-brain analysis of correlation within the PD cohort between individuals' UPDRS III score progression for each body side (red—UPDRS RIGHT; yellow—UPDRS LEFT) and grey matter volume rate of change in akineto-rigid and tremor-dominant forms of PD. Statistical parametric maps with a threshold for presentation purposes at $p < 0.001$, uncorrected for multiple comparisons overlaid on standard T1-weighted image in standard Montreal Neurological Institute space. Bottom: Bar plots represent the contrast estimates for each subgroup of PD patients. Middle—scatter plot of correlation between residuals (betas) of left motor cortex rate of change and right-sided ΔUPDRS III. Abbreviations: ΔUPDRS—bodyside specific change in the unified Parkinson's disease rating scale; AR_L—akineto-rigid symptoms on the left; AR_R—akineto-rigid symptoms on the right; TD_L—tremor-predominance on the left; TD_R—tremor-predominance on the right.

Table 3. Correlation between rate of gray matter volume change and UPDRS difference between time points.

Correlation	Region	Side	MNI Coordinates (mm)			*p*-Value (FWE-Corr)
			x	y	z	
UPDRS_PD LEFT	Motor cortex—M1	R	62	−18	27	$p < 0.001$
	Angular gyrus	R	57	−54	27	$p = 0.035$
	Middle frontal gyrus	R	51	40	20	$p = 0.03$
UPDRS_PD RIGHT	Motor cortex—M1	L	62	−18	38	$p = 0.028$
	Angular gyrus	L	−33	−60	33	$p = 0.03$
	Middle frontal gyrus	L	−42	36	35	$p = 0.05$

UPDRS improvement coded with positive values, deterioration coded with negative values.

4. Discussion

Our longitudinal study in PD patients demonstrates a specific pattern of progressive atrophy in cortical areas supporting motor and non-motor functions. Compared to an independent longitudinal dataset in healthy controls, we confirm the specificity of our findings as confined to PD rather than to processes related to ageing. The observed differences in the

rate of volume change that correlate in side-dependent manner with the motor symptom severity score emphasize the link between the dynamic assessment of brain atrophy and clinical progression. Conversely, the absence of significant interaction between PD clinical subtype and volume loss in the cerebellum support the notion of trait- rather than state-dependent differences between tremor-dominant and akineto-rigid forms of PD. These are novel findings that complement previous reports concerning longitudinal clinical and brain anatomy changes in idiopathic PD by offering robust measures of disease progression.

Our finding of the bilateral progressive atrophy of the anterior insula provides evidence for the importance of this structure in PD progression. We develop previous findings summarized in a meta-analysis of cross-sectional brain morphometry studies in PD [19] to demonstrate the temporal dynamics of anatomical changes in the insula as a major target of neurodegeneration [9,20,21]. The significance of the finding is underlined by the implication of a wider network of progressive atrophy, including the parahippocampal gyrus, precuneus and medial temporal gyrus—structures that are structurally and functionally strongly connected with the insula [22,23].

Our MRI data pre-processing strategy, featuring precision in assessing longitudinal volume changes and using high-dimensional diffeomorphic registration [16], provides strong support for previous tensor-based morphometry findings of changes in early PD patients [10]. The observed pattern of progressive atrophy follows the postulated trajectory of Lewy body pathology [24], which also corroborates recent findings on the grey matter loss correlates of CSF tau levels in PD [25]. The assumption here is that these changes represent the morphological correlates of progressive neuronal loss in the dopaminergic nigro-striatal system in mild to moderate PD patients. We can only speculate about the precise neurobiological process underlying the observed volume trajectories. The prevalent concept is that in PD, α-synuclein aggregates in cerebellar glia and Purkinje cells, but the temporal dynamics and spatial pattern of these accumulations with respect to disease stage and clinical correlate remain yet to be identified. This uncertainty is reflected in the controversial results demonstrated in PD patients but presumably reflects the different nature of the morphological changes.

For the purpose of the study, we separated patients based on the predominantly affected body side and according to tremor or akineto-rigid clinical subtype. We could not find strong supportive evidence for our hypothesis that tremor-dominant PD [26] has a benign disease course compared to the akineto-rigid subgroup [27,28]. Along the same lines, the trend for cerebellar differences in patients with tremor appear static, which hints towards involvement in the genesis of tremor rather than reflecting a neurodegenerative process [18]. Our findings of lateralized motor cortex atrophy over time, which depends in mirror-like manner on the UPDRS scores of the ipsi- and contralateral body, did not demonstrate any differences between tremulous and akineto-rigid forms of PD, which we interpret in light of the similar clinical progression of the two PD forms, which impacts the motor system in a state-dependent manner.

All PD subgroups had a similar demographic, clinical and neuropsychological profiles, except for more prevalent balance impairment and motor fluctuations and dyskinesias in the patients without tremor [18]. There is a low probability that these differences confounded our findings, since motor fluctuations and dyskinesias presumably originate from long-lasting functional alterations without known structural abnormalities. In this context, impaired balance and the eventual loss of postural stability in PD is primarily caused by the degeneration of brainstem nuclei, such as the tegmental pedunculo-pontine nucleus [29]. The dependence of these MRI parameters on different histological tissue properties hinders the interpretation of computational anatomy results at the microstructural level. The alternative hypothesis is that the observed pattern of changes in areas involved in associative and brain homeostatic functions represent compensatory responses to altered motor and non-motor behavior or remnants from asymptotic non-linear initial changes affecting the whole brain.

The shortcomings of this study include the current spatial resolution of MRI precluding the differentiation of small brain structures, particularly in the brainstem and thalamus. Considering various methodological limitations for the reliable detection of thalamus when using T1-weighted MRI [30], we may have missed thalamus changes over time, as reported in a previous study [31]. Additionally, we acknowledge the potential limitations that may have induced bias—first, that healthy volunteers' data were acquired in different studies with different inclusion and exclusion criteria, scanner types and sequences, and second, the inclusion of females in the control group, while the PD patients were only male. Despite these limitations, the robust morphometry findings in a cohort of moderate sample size compared with the numbers in the PPMI registry gives us confidence in the validity of our findings. Similarly, as already exemplified with ADNI data and as is becoming standard practice in imaging neuroscience, the pooling of structural MRI data from different scanners does not obscure the impact of neurodegeneration on brain anatomy.

The demonstrated unique pattern of cortical and subcortical changes confirms the long-standing notion of progressive brain anatomy changes in the due course of PD. Our findings can be interpreted in the context of clinical phenotype-specific atrophy and tested in the future as a non-invasive objective tool for monitoring the benefits of novel treatment strategies.

Supplementary Materials: The following supporting information can be downloaded at: https://www.mdpi.com/article/10.3390/ctn7010008/s1, Figure S1: Whole-brain analysis of grey matter volume differences between akineto-rigid and tremor-dominant forms of PD; Table S1: Main effects analysis—volume differences; Table S2: Main effects analysis after exclusion of female healthy controls—rate of gray matter volume change.

Author Contributions: D.H.B. designed the study, collected the data and performed the MRI procedure with J.v.M. and S.S.K. D.H.B., J.D. and B.D. conducted the data analysis. D.H.B., C.L.B., K.I. and B.D. wrote the manuscript. All authors have read and agreed to the published version of the manuscript.

Funding: This research project received no external funding.

Institutional Review Board Statement: The study was conducted in accordance with the Declaration of Helsinki, and approved by the Ethics Committee of the University of Zurich, Switzerland, 2005.

Informed Consent Statement: Informed consent was obtained from all subjects involved in the study.

Data Availability Statement: The data presented in this study are available on request from the corresponding authors. The data are not publicly available due to privacy and ethical reasons.

Acknowledgments: D.H.B. is supported by the Foundation Parkinson Switzerland and the Swiss National Science Foundation (320030E_192211/1) and holds the Baasch-Medicus Prize. B.D. is supported by the Swiss National Science Foundation (project grants Nr. 32003B_135679, 32003B_159780, 324730_192755 and CRSK−3_190185), ERA_NET iSEE project, the Swiss Personalised Health Network SACR project and the Leenaards Foundation. LREN is very grateful to the Roger De Spoelberch and Partridge Foundations for their generous financial support.

Conflicts of Interest: The authors have no competing financial interests.

References

1. Postuma, R.B.; Berg, D.; Stern, M.; Poewe, W.; Olanow, C.W.; Oertel, W.; Obeso, J.; Marek, K.; Litvan, I.; Lang, A.E.; et al. MDS clinical diagnostic criteria for Parkinson's disease. *Mov. Disord.* **2015**, *30*, 1591–1601. [CrossRef] [PubMed]
2. Schneider, S.A.; Obeso, J.A. Clinical and pathological features of Parkinson's disease. *Curr. Top. Behav. Neurosci.* **2015**, *22*, 205–220. [PubMed]
3. Draganski, P.B.; Accolla, E.A. Morphometric Analyses in Movement Disorders. In *Neuroimaging of Movement Disorders*; Nahab, F.B., Hattori, N., Eds.; Humana Press: Totowa, NJ, USA, 2013; pp. 25–47.
4. Gee, M.; Dukart, J.; Draganski, B.; Wayne Martin, W.R.; Emery, D.; Camicioli, R. Regional volumetric change in Parkinson's disease with cognitive decline. *J. Neurol. Sci.* **2017**, *373*, 88–94. [CrossRef] [PubMed]

5. Uribe, C.; Segura, B.; Baggio, H.C.; Abos, A.; Marti, M.J.; Valldeoriola, F.; Compta, Y.; Bargallo, N.; Junque, C. Patterns of cortical thinning in nondemented Parkinson's disease patients. *Mov. Disord.* **2016**, *31*, 699–708. [CrossRef] [PubMed]
6. Mak, E.; Su, L.; Williams, G.B.; Firbank, M.J.; Lawson, R.A.; Yarnall, A.J.; Duncan, G.W.; Owen, A.M.; Khoo, T.K.; Brooks, D.J.; et al. Baseline and longitudinal grey matter changes in newly diagnosed Parkinson's disease: ICICLE-PD study. *Brain J. Neurol.* **2015**, *138 Pt 10*, 2974–2986. [CrossRef]
7. Hanganu, A.; Bedetti, C.; Degroot, C.; Mejia-Constain, B.; Lafontaine, A.L.; Soland, V.; Chouinard, S.; Bruneau, M.-A.; Mellah, S.; Belleville, S.; et al. Mild cognitive impairment is linked with faster rate of cortical thinning in patients with Parkinson's disease longitudinally. *Brain J. Neurol.* **2014**, *137 Pt 4*, 1120–1129. [CrossRef]
8. Segura, B.; Baggio, H.C.; Marti, M.J.; Valldeoriola, F.; Compta, Y.; Garcia-Diaz, A.I.; Vendrell, P.; Bargallo, N.; Tolosa, E.; Junque, C. Cortical thinning associated with mild cognitive impairment in Parkinson's disease. *Mov. Disord.* **2014**, *29*, 1495–1503. [CrossRef]
9. Pieperhoff, P.; Südmeyer, M.; Dinkelbach, L.; Hartmann, C.J.; Ferrea, S.; Moldovan, A.S.; Minnerop, M.; Diaz-Pier, S.; Schnitzler, A.; Amunts, K. Regional changes of brain structure during progression of idiopathic Parkinson's disease—A longitudinal study using deformation based morphometry. *Cortex J. Devoted Study Nerv. Syst. Behav.* **2022**, *151*, 188–210. [CrossRef]
10. Tessa, C.; Lucetti, C.; Giannelli, M.; Diciotti, S.; Poletti, M.; Danti, S.; Baldacci, F.; Vignali, C.; Bonuccelli, U.; Mascalchi, M.; et al. Progression of brain atrophy in the early stages of Parkinson's disease: A longitudinal tensor-based morphometry study in de novo patients without cognitive impairment. *Hum. Brain Mapp.* **2014**, *35*, 3932–3944. [CrossRef]
11. Menke, R.A.L.; Szewczyk-Krolikowski, K.; Jbabdi, S.; Jenkinson, M.; Talbot, K.; Mackay, C.E.; Hu, M. Comprehensive morphometry of subcortical grey matter structures in early-stage Parkinson's disease. *Hum. Brain Mapp.* **2014**, *35*, 1681–1690. [CrossRef]
12. Ashburner, J.; Csernansky, J.G.; Davatzikos, C.; Fox, N.C.; Frisoni, G.B.; Thompson, P.M. Computer-assisted imaging to assess brain structure in healthy and diseased brains. *Lancet Neurol.* **2003**, *2*, 79–88. [CrossRef]
13. Hallgren, B.; Sourander, P. The effect of age on the non-haemin iron in the human brain. *J. Neurochem.* **1958**, *3*, 41–51. [CrossRef]
14. Gibb, W.R. Accuracy in the clinical diagnosis of parkinsonian syndromes. *Postgrad. Med. J.* **1988**, *64*, 345–351. [CrossRef]
15. Lorio, S.; Fresard, S.; Adaszewski, S.; Kherif, F.; Chowdhury, R.; Frackowiak, R.S.; Ashburner, J.; Helms, G.; Weiskopf, N.; Lutti, A.; et al. New tissue priors for improved automated classification of subcortical brain structures on MRI. *NeuroImage* **2016**, *130*, 157–166. [CrossRef]
16. Ashburner, J.; Ridgway, G.R. Symmetric diffeomorphic modeling of longitudinal structural MRI. *Front. Neurosci.* **2012**, *6*, 197. [CrossRef]
17. Ashburner, J. A fast diffeomorphic image registration algorithm. *NeuroImage* **2007**, *38*, 95–113. [CrossRef]
18. Benninger, D.H.; Thees, S.; Kollias, S.S.; Bassetti, C.L.; Waldvogel, D. Morphological differences in Parkinson's disease with and without rest tremor. *J. Neurol.* **2009**, *256*, 256–263. [CrossRef]
19. Pan, P.L.; Song, W.; Shang, H.F. Voxel-wise meta-analysis of gray matter abnormalities in idiopathic Parkinson's disease. *Eur. J. Neurol.* **2012**, *19*, 199–206. [CrossRef]
20. Christopher, L.; Koshimori, Y.; Lang, A.E.; Criaud, M.; Strafella, A.P. Uncovering the role of the insula in non-motor symptoms of Parkinson's disease. *Brain* **2014**, *137*, 2143–2154. [CrossRef]
21. Criaud, M.; Christopher, L.; Boulinguez, P.; Ballanger, B.; Lang, A.E.; Cho, S.S.; Houle, S.; Strafella, A.P. Contribution of insula in Parkinson's disease: A quantitative meta-analysis study. *Hum. Brain Mapp.* **2016**, *37*, 1375–1392. [CrossRef]
22. Chikama, M.; McFarland, N.R.; Amaral, D.G.; Haber, S.N. Insular cortical projections to functional regions of the striatum correlate with cortical cytoarchitectonic organization in the primate. *J. Neurosci.* **1997**, *17*, 9686–9705. [CrossRef] [PubMed]
23. Cauda, F.; Costa, T.; Torta, D.M.; Sacco, K.; D'agata, F.; Duca, S.; Geminiani, G.; Fox, P.T.; Vercelli, A. Meta-analytic clustering of the insular cortex: Characterizing the meta-analytic connectivity of the insula when involved in active tasks. *Neuroimage* **2012**, *62*, 343–355. [CrossRef] [PubMed]
24. Braak, H.; Del Tredici, K.; Rüb, U.; de Vos, R.A.I.; Jansen Steur, E.N.H.; Braak, E. Staging of brain pathology related to sporadic Parkinson's disease. *Neurobiol. Aging* **2003**, *24*, 197–211. [CrossRef]
25. Mak, E.; Su, L.; Williams, G.B.; Firbank, M.J.; Lawson, R.A.; Yarnall, A.J.; Duncan, G.W.; Mollenhauer, B.; Owen, A.M.; Khoo, T.K.; et al. Longitudinal whole-brain atrophy and ventricular enlargement in nondemented Parkinson's disease. *Neurobiol. Aging* **2017**, *55*, 78–90. [CrossRef] [PubMed]
26. Jankovic, J.; McDermott, M.; Carter, J.; Gauthier, S.; Goetz, C.; Golbe, L.; Huber, S.; Koller, W.; Olanow, C.; Shoulson, I.; et al. Variable expression of Parkinson's disease: A base-line analysis of the DATATOP cohort. The Parkinson Study Group. *Neurology* **1990**, *40*, 1529–1534. [CrossRef]
27. Marras, C.; Rochon, P.; Lang, A.E. Predicting motor decline and disability in Parkinson disease: A systematic review. *Arch. Neurol.* **2002**, *59*, 1724–1728. [CrossRef]
28. Josephs, K.A.; Matsumoto, J.Y.; Ahlskog, J.E. Benign tremulous parkinsonism. *Arch. Neurol.* **2006**, *63*, 354–357. [CrossRef]
29. Pahapill, P.A.; Lozano, A.M. The pedunculopontine nucleus and Parkinson's disease. *Brain J. Neurol.* **2000**, *123 Pt 9*, 1767–1783. [CrossRef]

30. Lorio, S.; Lutti, A.; Kherif, F.; Ruef, A.; Dukart, J.; Chowdhury, R.; Frackowiak, R.; Ashburner, J.; Helms, G.; Weiskopf, N.; et al. Disentangling in vivo the effects of iron content and atrophy on the ageing human brain. *Neuroimage* **2014**, *103*, 280–289. [CrossRef]
31. Kassubek, J.; Juengling, F.D.; Hellwig, B.; Spreer, J.; Lücking, C.H. Thalamic gray matter changes in unilateral Parkinsonian resting tremor: A voxel-based morphometric analysis of 3-dimensional magnetic resonance imaging. *Neurosci. Lett.* **2002**, *323*, 29–32. [CrossRef]